MITORIBOSOME

Molecular basis of translation termination at noncanonical stop codons in human mitochondria

Martin Saurer[1], Marc Leibundgut[1], Hima Priyanka Nadimpalli[2], Alain Scaiola[1], Tanja Schönhut[1], Richard G. Lee[3,4,5], Stefan J. Siira[3,4], Oliver Rackham[3,4,5,6], René Dreos[2], Tea Lenarčič[1], Eva Kummer[7], David Gatfield[2], Aleksandra Filipovska[3,4,5]*, Nenad Ban[1]*

The genetic code that specifies the identity of amino acids incorporated into proteins during protein synthesis is almost universally conserved. Mitochondrial genomes feature deviations from the standard genetic code, including the reassignment of two arginine codons to stop codons. The protein required for translation termination at these noncanonical stop codons to release the newly synthesized polypeptides is not currently known. In this study, we used gene editing and ribosomal profiling in combination with cryo–electron microscopy to establish that mitochondrial release factor 1 (mtRF1) detects noncanonical stop codons in human mitochondria by a previously unknown mechanism of codon recognition. We discovered that binding of mtRF1 to the decoding center of the ribosome stabilizes a highly unusual conformation in the messenger RNA in which the ribosomal RNA participates in specific recognition of the noncanonical stop codons.

Mitochondria maintain their own protein-synthesis machinery required to translate mRNAs transcribed from their highly reduced genome that encodes membrane proteins required for oxidative phosphorylation (OXPHOS) (*1*, *2*). Components of the mammalian mitochondrial translational machinery, such as mitochondrial ribosomes (mitoribosomes) (*3*, *4*), tRNAs, and protein factors, have diverged considerably from their bacterial predecessors (*5*, *6*). Furthermore, several changes to the standard genetic code have occurred in vertebrate mitochondria, including the emergence of unconventional stop codons (*1*, *7*).

Most prokaryotic and eukaryotic translation systems use the stop codons UGA, UAG, and UAA, which are recognized by release factors to terminate protein synthesis. Release factors recognize stop codons in the A-site of the small ribosomal subunit (SSU) to hydrolyze the ester bond between the P-site tRNA and the nascent polypeptide chain in the active site of the large ribosomal subunit (LSU) (*8*–*11*). In human mitochondria, UAG and UAA have retained their function as stop codons, whereas UGA encodes tryptophan (*1*, *12*). Furthermore, two additional stop codons, AGA and AGG, have emerged from reassigned arginine codons and are found at the end of the cytochrome C oxidase subunit 1 (COX1) and the nicotinamide adenine dinucleotide (reduced) (NADH)–ubiquinone oxidoreductase chain 6 protein (ND6) open reading frames (ORFs), respectively (*7*).

In bacteria, the stop codons UAG and UAA are recognized by release factor 1 (RF1), whereas UGA and UAA are read by release factor 2 (RF2) (*9*–*11*). In cytoplasmic translation, eukaryotes use a single factor, eRF1, that binds to all three stop codons (*8*). In human mitochondria, mitochondrial release factor 1a (mtRF1a or mtRF1L) releases ribosomes at UAG or UAA stop codons (*13*–*15*), yet it does not recognize the two noncanonical stop codons AGA and AGG (*13*, *14*) (Fig. 1A). Therefore, which factor releases nascent chains at noncanonical stop codons has remained elusive (*16*). Among previously considered candidates were the mitochondrial release factors ICT1 (mL62, MRPL58) and mtRF-R (C12ORF65) (*13*, *17*–*19*); however, it was subsequently established that they are responsible for the rescue of stalled mitoribosomes on truncated mRNAs or after aberrant translation termination (*8*, *13*, *18*, *20*). It was also proposed that termination at noncanonical stop codons in human mitochondria occurs by mtRF1a, following a −1 ribosomal frameshifting event (*21*). Lastly, mtRF1 was identified as a release factor on the basis of homology, but it was predicted that mtRF1 would not be able to bind to the decoding center because it contains sequence insertions in the stop codon–recognition domain that would prevent interactions with the mRNA (*22*, *23*). Several in vitro studies did not detect binding of mtRF1 to ribosomes programmed with AGA or AGG codons (*13*, *15*, *17*, *19*, *24*). Recently, mtRF1 has been shown to participate in the translation termination of COX1 but not of ND6; however, the mechanistic role of the factor in translation termination remained elusive (*25*).

In this study, we used biochemical and structural approaches to establish that mtRF1 is responsible for termination at noncanonical stop codons in human mitochondria. We also show that the specific recognition of the stop codon occurs through a network of interactions between the codon, mtRF1, and the ribosomal RNA (rRNA).

Results and discussions

mtRF1 is required for translation termination of COX1

It is currently unclear which factor is responsible for the release at noncanonical stop codons. We used genome editing to delete each of the four mitochondrial release factors mtRF1, mtRF1a, mtRF-R, and ICT1, as well as for the simultaneous deletion of both mtRF1 and mtRF1a in human CAL51 cells. Loss of mtRF1 led to a reduction of the steady state (Fig. 1B) and de novo synthesis (Fig. 1C) of the mitochondrially encoded polypeptide COX1, whereas loss of mtRF1a and the double deletion ("knockout," KO) of mtRF1 and mtRF1a caused global reduction in mitochondrial protein synthesis (Fig. 1C). This indicates that mtRF1 is specifically required for efficient translation termination of COX1. The observed residual production of COX1 in the absence of mtRF1 (Fig. 1C) is likely because of the activity of rescue factor mtRF-R (*20*, *25*). Deletion of mtRF-R or ICT1 resulted in marked and general reduction of mitochondrial protein synthesis (fig. S1A), which was consistent with their role as rescue factors in translation (*15*, *20*). COX1 is needed for the initial assembly of the catalytic core of the OXPHOS complex IV, and diminished levels of COX1 are likely to disrupt complex IV assembly and reduce the stability of members of complex IV (*26*). Accordingly, we observed reduced steady-state abundance of COX2 in mtRF1-KO cells (Fig. 1B). The decreased levels of complex IV proteins in the absence of mtRF1 resulted in reduced mitochondrial respiration (fig. S1B). Moreover, we conducted ribosome footprinting experiments (*27*, *28*), which identified that loss of mtRF1 leads to the stalling of mitoribosomes on the noncanonical stop codons at the end of the COX1 and ND6 mRNAs (Fig. 1, D and E), but generally not on the canonical stop codons UAA and UAG (fig. S2). Codon occupancy analyses further corroborated the increased stalling of mitoribosomes at noncanonical codons AGA and AGG in the mtRF1-KO cells (Fig. 1F). These results reveal that noncanonical AGA or AGG termination at the end of COX1 and ND6 genes is specifically compromised in the absence of mtRF1. Next, we addressed whether the catalytic activity of

[1]Department of Biology, Institute of Molecular Biology and Biophysics, ETH Zürich, 8093 Zürich, Switzerland. [2]Center for Integrative Genomics, University of Lausanne, 1015 Lausanne, Switzerland. [3]Harry Perkins Institute of Medical Research, The University of Western Australia, Nedlands, Western Australia 6009, Australia. [4]ARC Centre of Excellence in Synthetic Biology, QEII Medical Centre, The University of Western Australia, Nedlands, Western Australia 6009, Australia. [5]Telethon Kids Institute, Northern Entrance, Perth Children's Hospital, 15 Hospital Avenue, Nedlands, Western Australia, Australia. [6]Curtin Medical School and Curtin Health Innovation Research Institute, Curtin University, Bentley, Western Australia 6102, Australia. [7]Novo Nordisk Foundation Center for Protein Research, Protein Structure and Function Program, Blegdamsvej 3B, 2200 København N, Denmark.
*Corresponding author. Email: aleksandra.filipovska@uwa.edu.au (A.F.); ban@mol.biol.ethz.ch (N.B.)

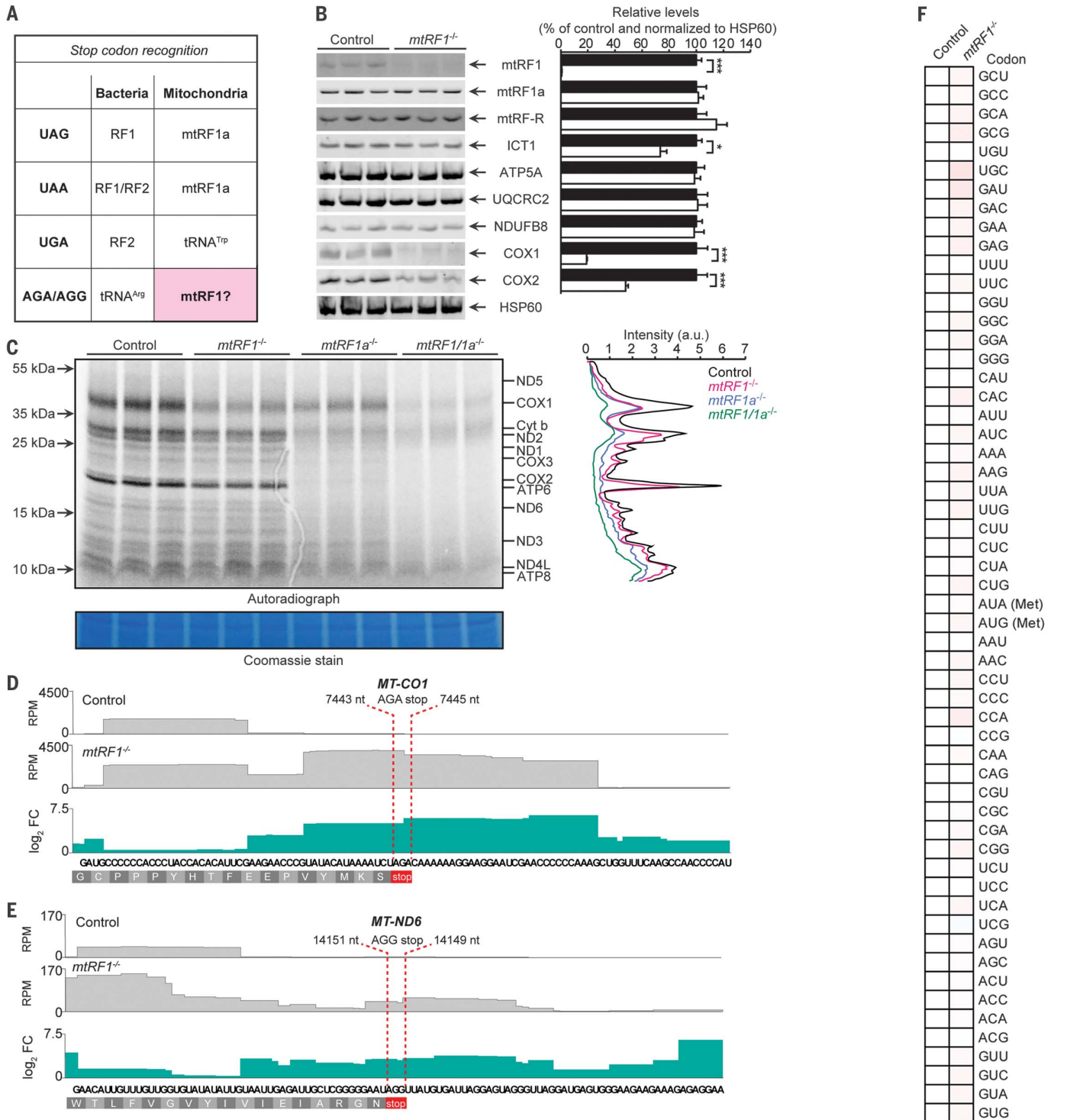

Fig. 1. Loss of mtRF1 reduces the translation of specific mitochondrially encoded mRNAs. (**A**) Comparison of stop-codon occurrence and recognition in bacteria and human mitochondria. (**B**) Immunoblotting against mitochondrial proteins in control and *mtRF1*$^{-/-}$ cells; HSP60 was used as a loading control. Relative abundance of proteins was measured with the Image Studio Lite 5.2 software and normalized to the loading control. Data are mean ± SEM. *$P < 0.05$; ***$P < 0.001$, determined using Student's *t* test. (**C**) De novo mitochondrial protein synthesis was measured by ^{35}S[methionine] and ^{35}S[cysteine] incorporation in control, *mtRF1*$^{-/-}$ and *mtRF1a*$^{-/-}$ cells ($n = 3$). 20 μg of cell lysates were separated by SDS-PAGE and visualized by autoradiography. Coomassie-stained gels are shown as loading controls. (**D** to **F**) Ribosomal profiling was carried out on translating mitoribosome fractions isolated from *mtRF1*$^{-/-}$ and control cells. Normalized read counts are shown in gray at the termination regions of *MT-CO1* (D) and *MT-ND6* (E) in *mtRF1*$^{-/-}$ and control cells, and the $\log_2$ fold-changes between them show increased (turquoise) and decreased (orange) coverage in specific regions of the mRNA ends. (F) Heatmap showing the $\log_2$ fold change difference in codon occupancy in the mtRF1 KO compared to control mitoribosome profiles. The $\log_2$ fold-change shown ranges from −10 to 10.

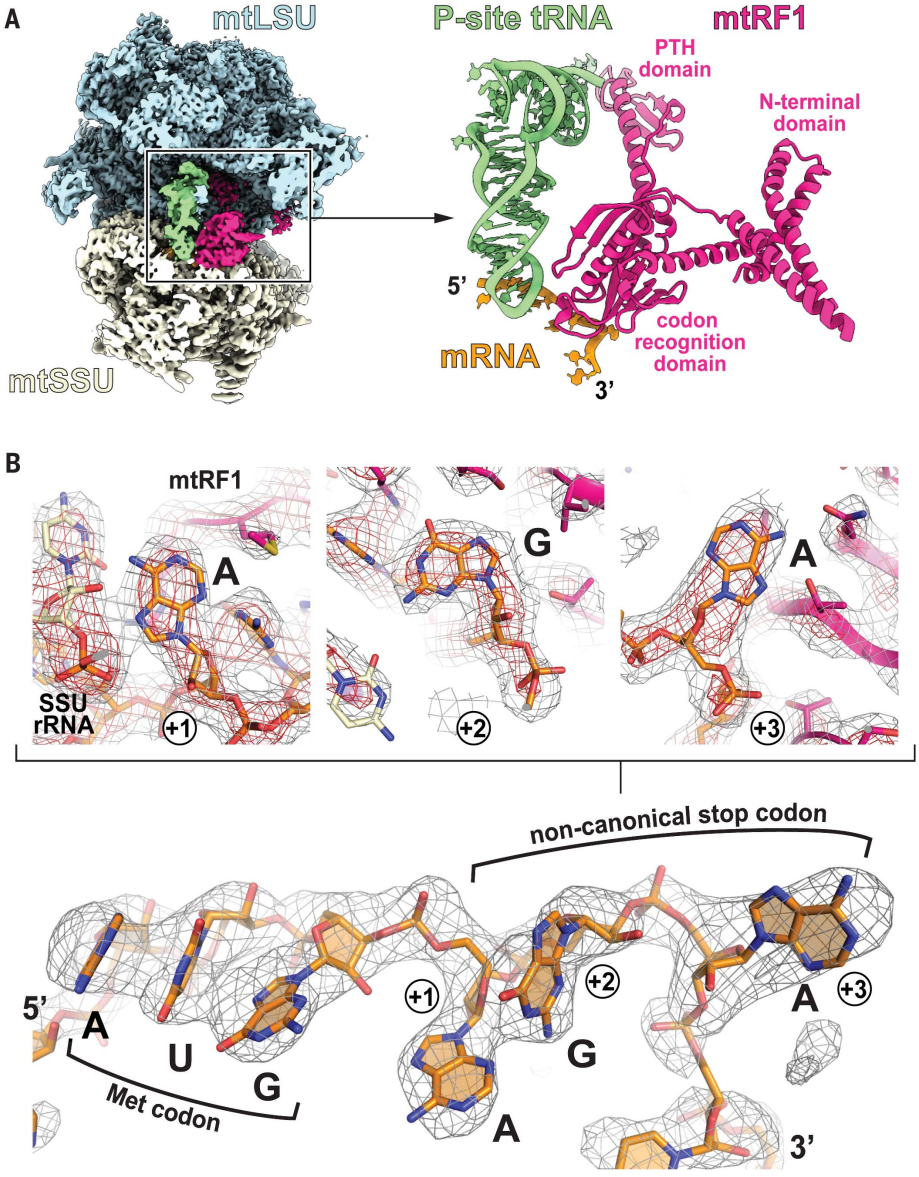

Fig. 2. Cryo-EM densities of the reconstituted mammalian mitoribosome–mtRF1^{wt} complex. (**A**) Overview of mtRF1 (magenta) bound to the A-site of the 55*S* mitoribosome with mRNA (orange) and tRNA^{Met} (green) in the P-site shown in the filtered cryo-EM reconstruction. A model of the visualized release factor, the mRNA, and the tRNA is shown in the same orientation. (**B**) Detailed views of cryo-EM densities that represent the noncanonical AGA stop codon in the mRNA shown at two different thresholds (gray and red). Whereas tRNA^{Met} base-pairs with the AUG codon in the P-site, the three purines of the noncanonical stop codon AGA interact with the codon recognition domain of mtRF1 in the A-site.

mtRF1 is required for translation termination. The activity of the conserved peptidyl-tRNA hydrolysis (PTH) domain of release factors can be suppressed by mutation of the catalytic GGQ motif to AAQ, which renders them unable to release the nascent chain (*8*). When expressed in *mtRF1*$^{-/-}$ cells, mtRF1^{AAQ} was not able to rescue translation of COX1 (fig. S1C), which indicates that the catalytic activity of mtRF1 is required for the synthesis of COX1. Concomitant with the strong decrease in COX1 levels in *mtRF1*$^{-/-}$ cells, we observed that mitochondrial protein biosynthesis was globally diminished, although to a lesser degree than COX1 itself. Conceivably, this global reduction was caused by a reduced pool of translation-competent mitoribosomes, because COX1 polypeptides cannot be efficiently released in the absence of mtRF1. These results show that mtRF1 is the release factor responsible for the recognition of noncanonical stop codons. This conclusion is supported by the work of two independent research groups who published their findings during the revision of this manuscript (*25*, *29*). However, these results also raise the question of how the unusual codon-recognition domain of mtRF1 accomplishes this task.

Structure determination of the mtRF1 termination complex

To gain insights into the mechanism of codon recognition by mtRF1, we solved the structure of an in vitro–reconstituted complex of the mitoribosome and mtRF1 by single-particle cryo-EM. Human embryonic kidney 293 (HEK293) cells were transfected with a plasmid that encoded the human wild-type (WT) mtRF1 protein with a C-terminal FLAG tag. Following the isolation and lysis of mitochondria, mtRF1^{wt}-FLAG was affinity-purified with anti-FLAG resin. Mitoribosomal subunits were purified from pig liver tissue and combined with a short mRNA (5′-A AUG AGA CAA-3′) and the human mitochondrial formylmethionine (fMet)–tRNA^{Met} to obtain translation termination complexes with the noncanonical stop codon AGA in the A-site of the mitoribosome. Purified mtRF1^{wt}-FLAG was added and after a short incubation, the mixture was prepared for analysis by single-particle cryo-EM. We found 55*S* mitoribosomes with bound mRNA, the tRNA in the P-site, and mtRF1 bound to the A-site. We were able to calculate a map for this complex that reached an overall resolution of 3.6 Å, and additional refinement focused on either the SSU- or the LSU-yielded maps at overall resolutions of 3.6 Å and 3.5 Å, respectively (Fig. 2 and figs. S3 and S4). To build an atomic model for mtRF1, we used an AlphaFold2 model (*30*) and a recently published structure of mtRF1a (*13*) as a guide.

mtRF1 binds to a highly distorted mRNA conformation

Although mtRF1 and mtRF1a share a similar fold, regions with considerable differences can be found in the N-terminal domain, where an extension containing positively charged amino acids is found in mtRF1 (Fig. 3, A and C, and fig. S5A). In our reconstruction, we see this extension protruding into a pocket below the L7/L12 stalk of the LSU that is formed by the tips of helices of the LSU rRNA, which is an interaction that might help to stabilize mtRF1 binding (Fig. 2A).

Whereas the catalytic PTH domain of mtRF1 that releases the peptide in the active site of the ribosome is highly conserved, the codon-recognition domain features insertions at the tip of helix α5 and in the codon-recognition loop that are incompatible with canonical codon recognition by mtRF1 (Fig. 3). The two additional amino acids (threonines 194 and 195) extend the tip of helix α5 in the A-site of the SSU, thereby distorting the mRNA backbone and reorienting the first two bases of the noncanonical stop codon (Fig. 3B). The structure of the codon-recognition loop also markedly differs from canonical mtRF1a because it

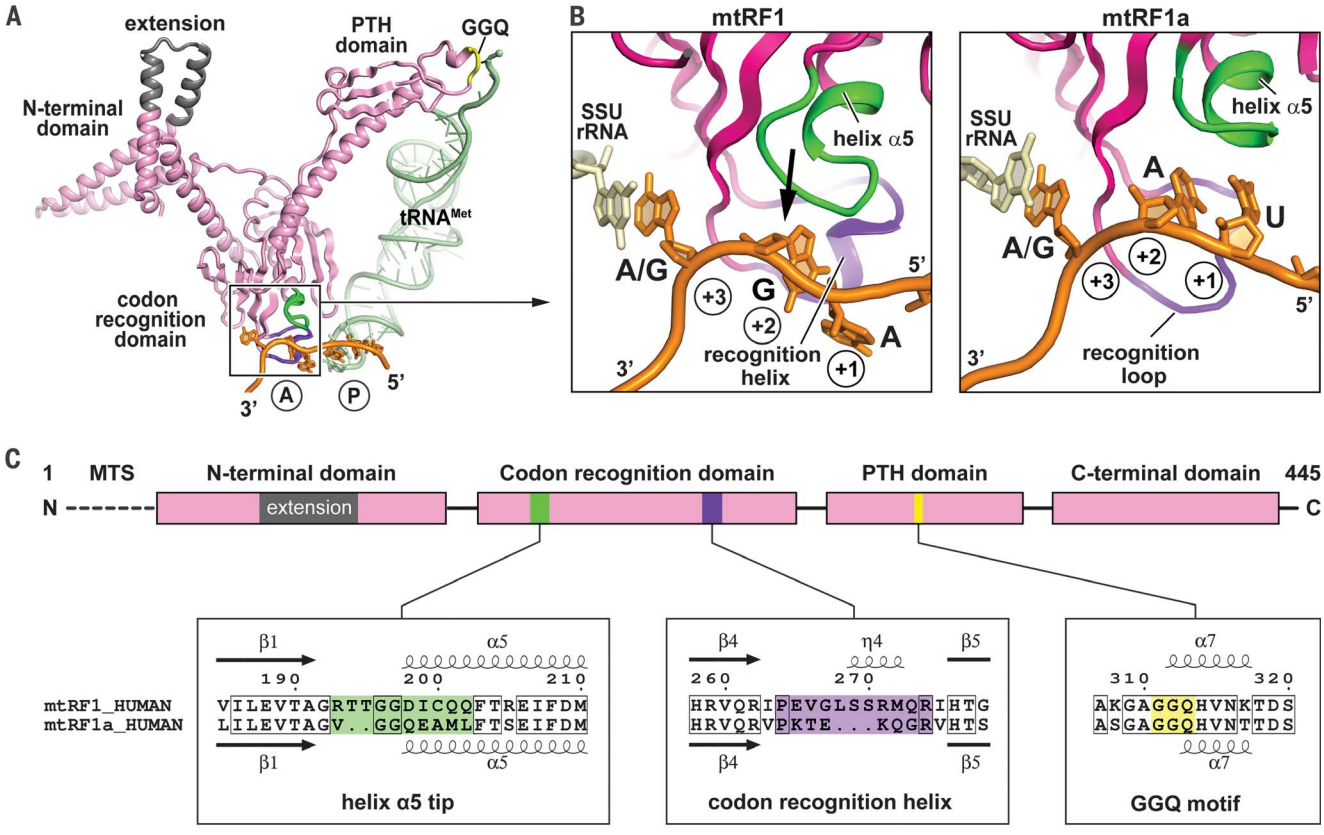

Fig. 3. Comparison between the mRNA recognition in the A-site of the SSU by the noncanonical mtRF1 and the canonical mitochondrial release factor mtRF1a. (**A**) Overview of release factor mtRF1 (pink) bound to mRNA (orange) in the A-site of the decoding center in the SSU, with $tRNA^{Met}$ in the P-site. The extension of the N-terminal domain is highlighted in gray. The location of the catalytic GGQ motif is shown in yellow. (**B**) Detailed view of the A-site of mtRF1 (this study) and comparison with mtRF1a (*13*). The loop-preceding helix α5 (green) is extended in mtRF1 and pushes the purine bases at the first two positions away from the recognition helix (purple), whereas in mtRF1a, the corresponding bases are embraced by the recognition loop. The purine in the third position is held in a similar position by amino acids that are conserved in both factors, as well as by a stacking base of the rRNA. (**C**) Schematic domain overview of mtRF1. Alignments between the functionally important regions of mtRF1 and mtRF1a are shown below. MTS, mitochondrial targeting sequence. Single-letter abbreviations for the amino acid residues are as follows: A, Ala; C, Cys; D, Asp; E, Glu; F, Phe; G, Gly; H, His; I, Ile; K, Lys; L, Leu; M, Met; N, Asn; P, Pro; Q, Gln; R, Arg; S, Ser; T, Thr; V, Val; W, Trp; and Y, Tyr.

forms a short α-helix with several key residues oriented toward the first and second base of the noncanonical stop codon (Fig. 3B and fig. S5). Consequently, we refer to it as the "recognition helix." Instead of embracing the codon in the same way that the recognition loop of mtRF1a does, the recognition helix of mtRF1 pushes the first two bases of the codon away such that they point toward the head of the SSU (Fig. 3B). Binding of mtRF1 further results in a distortion in helix 44 of the SSU rRNA, with the decoding bases alternatively flipped (fig. S6).

As an independent validation, we solved the structure of the human translation termination complex purified from mitochondria. We expressed FLAG-tagged, catalytically defective mutant $mtRF1^{AAQ}$ in HEK293 cells to affinity-purify stalled noncanonical termination complexes for structure determination by cryo-EM. The obtained reconstruction of the human termination complex at 3.0 Å overall resolution (figs. S7 to S9) revealed the same conformation of the mRNA and of the codon-recognition domain of $mtRF1^{AAQ}$ as in the in vitro–reconstituted complex. On the basis of the visual inspection of the densities of the mRNA and the P-site tRNA, we could establish that the ribosomes contained the mRNA sequence AU(G/A)AG(G/A) with $tRNA^{Met}$ in the P-site interacting with AU(G/A) and the release factor interacting with AG(G/A) (figs. S9 and S10). Because these sequences neither correspond to the end of the *MT-COX1* nor to the *MT-ND6* ORFs, we performed ribosome profiling on pulled-down $mtRF1^{AAQ}$ complexes to identify which sequences the ribosomes may be interacting with. In addition, we also profiled whole mitochondria from $mtRF1^{AAQ}$-expressing cells to evaluate the specificity of the obtained footprint signals. This analysis revealed ribosome footprints at several AU(G/A)AG(G/A) sites located on the (+) strand transcript, two of which were located in the −1 frame within *MT-ND4* (fig. S11, C and D) and one in the −1 frame within *MT-ND5* (fig. S11, C and E). In comparison with whole-mitochondria footprints, a local peak in coverage on these sites was apparent in pulled-down $mtRF1^{AAQ}$-complex data. The preferential identification of complexes with $tRNA^{Met}$ in the P-site of the mitoribosome may be explained by the conserved, stabilizing features of its anticodon stem-loop (*31*) and the availability of AU(G/A)AG(G/A) sites located outside of known reading frames (fig. S11).

mtRF1 recognizes noncanonical stop codons with help from rRNA

The structures of translation termination complexes allowed us to establish the chemical basis of stop-codon recognition. The distortion of the mRNA that occurs owing to the unusual structure of the mtRF1 codon-recognition domain positions the noncanonical stop codons such that they are specifically recognized by a combination of chemical features in mtRF1, the surrounding bases of the SSU rRNA, and neighboring bases of the mRNA. We describe

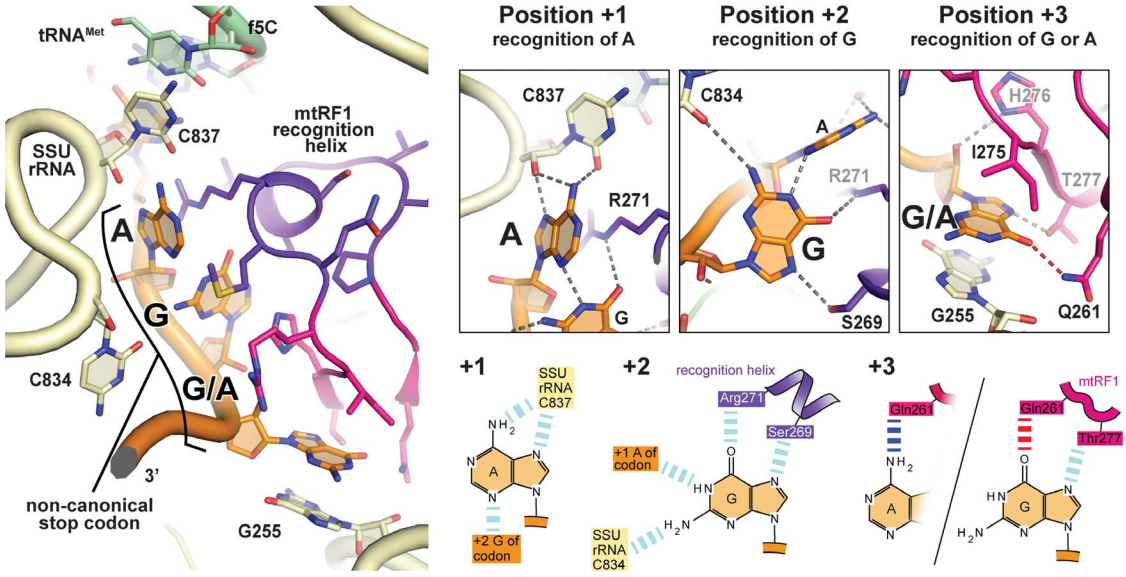

Fig. 4. The structural basis of noncanonical stop codon recognition. The A-site of the human mitoribosome in complex with mtRF1 is shown. A network of interactions that includes residues of mtRF1, the SSU rRNA, and the mRNA itself define the identity of the first two purine bases as A and G, respectively, whereas at the third position, both purine bases can be specifically recognized. Important interactions at all three stop codon positions are shown in detailed views, with corresponding schematics below.

these interactions as visualized for the human translation-termination complex.

The adenosine at the first position is stabilized by stacking onto arginine 271 of the codon-recognition helix (Fig. 4 and fig. S5F). In this orientation, the Hoogsteen edge of the adenosine forms hydrogen bonds with the sugar edge of cytosine C837 (human nomenclature) of the SSU rRNA. Owing to the number of possible hydrogen bonds and the complementary partial charges, adenosine is favored in this position over all other bases. In particular, the carbonyl group of guanosine, the other purine, would not be able to form favorable interactions with C837. In this way, mtRF1 does not directly detect the identity of the first base through amino acid side chains; rather, the helix α5 loop and the codon-recognition loop orient the first base such that it forms specific hydrogen bonds with the rRNA only in case of an adenosine as the first base.

The side chain of arginine 271 is also involved in the recognition of the base in the +2 position. Its positively charged guanidinium group interacts with the carbonyl group of the +2 guanosine, thereby arranging the guanosine almost perpendicularly relative to the +1 adenosine (Fig. 4). This conformation allows a hydrogen bond to form between the N1 atom of guanosine and the N3 atom of the +1 adenosine. As is the case for the first adenosine, a base of the SSU rRNA is also involved in the recognition of the second guanosine: The amino group of the guanosine faces the 2-hydroxyl group of C834 (human nomenclature) and form a hydrogen bond. Additionally, the +2 guanosine is sterically hindered from rotating away by the extended loop at the tip of helix α5 and an additional hydrogen bond with serine 269 that resides in the codon-recognition helix. Altogether, these extensive and specific interactions strongly favor a guanosine over all other bases in the second position.

In the third position of the A-site codon, both guanosine and adenosine can be recognized without any conformational changes of the factor or the mRNA. This is consistent with our observation that the structure of the in vivo–purified sample with a mixture of A and G in the third position was identical to the structure of the reconstituted complex that contained the AGA codon. The purine base at the last position of the stop codon is sandwiched between G255 (human nomenclature) of the SSU rRNA and isoleucine 275 of mtRF1 and is held in place by hydrogen bonds with threonine 277 and with the backbone carbonyl atom of isoleucine 275. Finally, both the carbonyl group of a guanosine or the amino group of an adenosine would be able to form hydrogen bonds with glutamine 261 depending on the orientation of the side chain. This mode of third-base recognition is highly similar to what was previously observed for mtRF1a and bacterial RF1, release factors that can recognize both G and A in the third position of stop codons (*10*, *13*, *32*). Therefore, mtRF1 recognizes both purines in the third position of the stop codon, which is in agreement with our observation that the stalling of mitoribosomes occurs at both noncanonical stop codons in the absence of mtRF1 (Fig. 1, D to F, and fig. S2).

In conclusion, our cryo-EM reconstructions reveal how mtRF1 interacts with noncanonical stop codons in a highly specific manner. In contrast with all other described release factors, mtRF1 has to recognize two stop codons with adenosine at the first position instead of uracil. To meet this requirement, mtRF1 has evolved a codon-recognition mechanism that is distinct from all other canonical release factors. Rather than identifying the codon in the A-site by direct interactions of amino acid side chains with the bases, as observed in bacterial RF1 and mtRF1a (*10*, *13*), mtRF1 repositions the first two bases of the stop codon to use an intricate network of interactions that includes residues of the release factor, the rRNA of the SSU, as well as neighboring bases of the mRNA. These interactions are only established if the identity of the first two bases is "AG," whereas both G and A are recognized in the third position. It follows that mtRF1 specifically recognizes the codons AGA and AGG and selects against all other sense or stop codons that are unable to form the observed network of interactions. The role of mtRF1 in translation termination on AGA and AGG codons is likely broadly conserved in vertebrates owing to a high level of sequence similarity in the key regions of the release factor involved in codon recognition (*32*). The results presented here reveal the molecular machinery that resulted from an extremely rare evolutionary recoding event, which affected codon usage across the entire genome and required replacement of a particular tRNA by a remodeled release factor.

REFERENCES AND NOTES

1. S. Anderson *et al.*, *Nature* **290**, 457–465 (1981).
2. O. Rackham, A. Filipovska, *Nat. Rev. Genet.* **23**, 606–623 (2022).
3. A. Amunts, A. Brown, J. Toots, S. H. W. Scheres, V. Ramakrishnan, *Science* **348**, 95–98 (2015).
4. B. J. Greber *et al.*, *Science* **348**, 303–308 (2015).
5. E. Kummer, N. Ban, *Nat. Rev. Mol. Cell Biol.* **22**, 307–325 (2021).
6. P. Bieri, B. J. Greber, N. Ban, *Curr. Opin. Struct. Biol.* **49**, 44–53 (2018).
7. S. Osawa, T. Ohama, T. H. Jukes, K. Watanabe, *J. Mol. Evol.* **29**, 202–207 (1989).
8. A. Brown, S. Shao, J. Murray, R. S. Hegde, V. Ramakrishnan, *Nature* **524**, 493–496 (2015).
9. A. Korostelev *et al.*, *Proc. Natl. Acad. Sci. U.S.A.* **105**, 19684–19689 (2008).
10. M. Laurberg *et al.*, *Nature* **454**, 852–857 (2008).
11. A. Weixlbaumer *et al.*, *Science* **322**, 953–956 (2008).

12. B. G. Barrell, A. T. Bankier, J. Drouin, *Nature* **282**, 189–194 (1979).
13. E. Kummer, K. N. Schubert, T. Schoenhut, A. Scaiola, N. Ban, *Mol. Cell* **81**, 2566–2582.e6 (2021).
14. Y. Nozaki, N. Matsunaga, T. Ishizawa, T. Ueda, N. Takeuchi, *Genes Cells* **13**, 429–438 (2008).
15. H. R. Soleimanpour-Lichaei *et al*., *Mol. Cell* **27**, 745–757 (2007).
16. F. Nadler, E. Lavdovskaia, R. Richter-Dennerlein, *RNA Biol.* **19**, 117–131 (2021).
17. S. Akabane, T. Ueda, K. H. Nierhaus, N. Takeuchi, *PLOS Genet.* **10**, e1004616 (2014).
18. H. A. Feaga, M. D. Quickel, P. A. Hankey-Giblin, K. C. Keiler, *PLOS Genet.* **12**, e1005964 (2016).
19. C. Lind, J. Sund, J. Aqvist, *Nat. Commun.* **4**, 2940 (2013).
20. N. Desai *et al*., *Science* **370**, 1105–1110 (2020).
21. R. Temperley, R. Richter, S. Dennerlein, R. N. Lightowlers, Z. M. Chrzanowska-Lightowlers, *Science* **327**, 301 (2010).
22. M. A. Huynen, I. Duarte, Z. M. Chrzanowska-Lightowlers, S. B. Nabuurs, *Biol. Direct* **7**, 14 (2012).
23. Y. Zhang, L. L. Spremulli, *Biochim. Biophys. Acta* **1443**, 245–250 (1998).
24. I. Duarte, S. B. Nabuurs, R. Magno, M. Huynen, *Mol. Biol. Evol.* **29**, 3497–3512 (2012).
25. F. Nadler *et al*., *Nat. Commun.* **13**, 6406 (2022).
26. S. Dennerlein, P. Rehling, *J. Cell Sci.* **128**, 833–837 (2015).
27. R. J. Morscher *et al*., *Nature* **554**, 128–132 (2018).
28. E. Schöller *et al*., *Mol. Cell* **81**, 4810–4825.e12 (2021).
29. A. Krüger *et al*., *Nat. Commun.* **14**, 30 (2023).
30. J. Jumper *et al*., *Nature* **596**, 583–589 (2021).
31. E. Kummer *et al*., *Nature* **560**, 263–267 (2018).
32. D. J. Young *et al*., *RNA* **16**, 1146–1155 (2010).

ACKNOWLEDGMENTS

We are grateful to the members of the Ban lab, in particular K. Schubert, A. Picenoni, R. Jost, and D. Yudin, for help with sample purification and helpful discussions. We thank M. Stentenbach from the Filipovska group for help with the respiration experiments. We are indebted to M. Peterek, B. Qureshi, D. Boehringer, and the ETH Scientific Center for Optical and Electron Microscopy (ScopeM) for support during cryo-EM data collection. **Funding:** Swiss National Science Foundation (SNSF) individual grant 179190 (D.G.); SNSF individual grants 31003A_182341 and 310030_212308 (N.B.); Swiss National Center of Competence in Research (NCCR), RNA & Disease program, project funding 141735 (D.G.), 51NF40-182880, and 51NF40-205601 (N.B.); Roessler Prize, Ernst Jung Prize, and Otto Naegeli Prize for Medical Research (N.B.); European Molecular Biology Organization (EMBO) long-term fellowship grant 1074-2019 (T.L.); National Health and Medical Research Council (NHMRC), Australian Research Council (ARC), Western Australian Child Research Fund (WACRF), and Cancer Council of Western Australia (CCWA) fellowships and project grants (O.R. and A.F.).
Author contributions: E.K. and T.L. carried out initial experiments. R.G.L., S.J.S., O.R., and A.F. carried out cell biology and *mtRF1*$^{-/-}$ ribo-profile experiments. M.S., T.S., and E.K. purified and prepared samples for cryo-EM studies. A.S. and M.S. collected and processed cryo-EM data. M.S. and M.L. performed molecular model building and refinement. M.S., M.L., and N.B. interpreted the density. H.P.N., R.D., and D.G. designed, executed, and interpreted the ribo-profile experiments with mitochondria and purified mitoribosomes from mtRF1^{AAQ}-expressing cells. M.S., M.L., and N.B. drafted the manuscript. H.P.N., A.S., R.G.L., S.J.S., O.R., R.D., E.K., T.L., D.G., and A.F. reviewed and edited the manuscript.
Competing interests: Authors declare that they have no competing interests. **Data and materials availability:** The coordinates and corresponding cryo-EM map of the in vitro reconstituted mammalian 55*S*-mtRF1^{wt}-mRNA-tRNA^{Met} complex are available in the Protein Data Bank (PDB) as PDB ID 8OIN and in the Electron Microscopy Data Bank (EMDB) as EMD-16894, respectively. The structures and maps focused on either the SSU (28S-mtRF1^{wt}-mRNA-tRNA^{Met}) or the LSU (39S-mtRF1^{wt}-tRNA^{Met}) are deposited under the accession codes PDB 8OIP and EMD-16895 and PDB 8OIQ and EMD-16896, respectively. The coordinates and corresponding cryo-EM map of the human 55*S*-mtRF1^{AAQ}-mRNA-tRNA^{Met} complex are available as PDB ID 8OIR and as EMD-16897, respectively. The structures and maps focused on either the SSU (28S-mtRF1^{AAQ}-mRNA-tRNA^{Met}) or the LSU (39S-mtRF1^{AAQ}-tRNA^{Met}) are deposited under the accession codes PDB 8OIS and EMD-16898, and PDB 8OIT and EMD-16899, respectively. Sequencing data for ribo-profiling from isolated mitochondria of control and mtRF1^{AAQ}-expressing cells have been deposited at Gene Expression Omnibus (GEO) GSE216779. Sequencing data for ribo-profiling from *mtRF1*$^{-/-}$ and control mitochondria have been deposited at GEO GSE216979.

SUPPLEMENTARY MATERIALS

science.org/doi/10.1126/science.adf9890
Materials and Methods
Figs. S1 to S11
Table S1 and S2
References (*33*–*61*)
MDAR Reproducibility Checklist

View/request a protocol for this paper from *Bio-protocol*.

Submitted 25 November 2022; accepted 1 April 2023
10.1126/science.adf9890